

Chemical evolution of Sagittarius: the heavy elements Eu and Ba

M. Molero^{1,2}, D. Romano³, M. Reichert⁴, F. Matteucci^{1,2,5}, A. Arcones^{6,7}, G. Cescutti^{1,2}, P. Simonetti², C. J. Hansen⁸ and G. A. Lanfranchi⁹

¹ Dipartimento di Fisica, Sezione di Astronomia, Università degli studi di Trieste, Via G.B. Tiepolo 11, I-34143 Trieste, Italy

² INAF, Osservatorio Astronomico di Trieste, Via Tiepolo 11, I-34131 Trieste, Italy

³ INAF, Osservatorio di Astrofisica e Scienza dello Spazio, Via Gobetti 93/3, I-40129 Bologna, Italy

⁴ Departament d'Astronomia i Astrofisica, Universitat de València

⁵ INFN, Sezione di Trieste, Via Valerio 2, I.34127 Trieste, Italy

⁶ Institut für Kernphysik, Technische Universität Darmstadt, Schlossgartenstr. 2, Darmstadt 64289, Germany

⁷ GSI Helmholtzzentrum für Schwerionenforschung GmbH, Planckstr. 1, Darmstadt 64291, Germany

⁸ Goethe University Frankfurt, Institute for Applied Physics, Max-von-Laue-Str. 12, 60438, Frankfurt am Main, Germany

⁹ Núcleo de Astrofísica, Universidade Cidade de São Paulo, R. Galvão Bueno 868, Liberdade, 01506-000, São Paulo, SP, Brazil
e-mail: marta.molero@phd.units.it

Received: 03-11-2022; Accepted: 13-01-2022

Abstract. We study the evolution of the europium (Eu) and barium (Ba) abundances in the Sagittarius dwarf spheroidal galaxy by means of a one-zone chemical evolution model which includes gas infall and outflow as well as detailed stellar nucleosynthesis. We test different scenarios for the production of r-process material, including merging neutron stars and magnetorotational-driven supernovae. The s-process material is instead assumed to be produced by low-intermediate mass stars during the asymptotic giant branch phase. Our simulations show that in order to reproduce the observed [Eu/Fe] vs [Fe/H] abundance pattern both a delayed and a quick source are necessary as r-process producers. In our model the delayed source is represented by neutron stars binary systems merging with a delay time distribution $\propto t^{-0.9}$, while the quick source is represented by magnetorotational driven supernovae. The yield of Eu from merging neutron stars should be in the $(3.0 \times 10^{-6} - 1.5 \times 10^{-5})M_{\odot}$ range, while that produced by magnetorotational-driven supernovae would be in the range of the theoretical calculations of Nishimura et al. (2017) and equal to $4.69 \times 10^{-7}M_{\odot}$. However, this same scenario fails in reproducing the observed abundance pattern of [Ba/Fe] vs [Fe/H], suggesting that more investigation is still needed in order to better constrain the origin of heavy elements.

Key words. stars: neutron – galaxies: abundances – galaxies: dwarf – galaxies: evolution

1. Introduction

The process responsible for the formation of heavy elements beyond the iron peak is neutron capture. It can be *slow* (s-process) or *rapid* (r-process) with respect to the β -decay in nuclei. Therefore, we are dealing with s-process or r-process elements.

The main s-process component takes place in the asymptotic giant branch (AGB) phase of low and intermediate mass stars (LIMS) (Busso et al., 1999), while the major astrophysical r-process site is still under debate, with possible candidate sites being supernovae or neutron star (NS) mergers (see e.g.: Thielemann et al., 2011; Frebel & Beers, 2018; Cowan et al., 2019).

Among massive stars, core-collapse supernovae (CC-SNe) induced by strong magnetic fields and/or fast rotation of the stellar core (magneto-rotational driven supernovae, MRD-SNe) seem to provide a source for the r-process (Winteler et al., 2012; Nishimura et al., 2015; Nishimura et al., 2017; Mösta et al., 2018; Halevi & Mösta, 2018; Reichert et al., 2021). However, the required rotation rates and magnetic energies restrict the mechanism to a minority of progenitor stars: only 1% of all stars with initial mass larger than $10 M_{\odot}$ may have the necessary conditions to host strong enough magnetic fields, according to Woosley & Heger (2006).

Merging neutron stars (MNS) have been supposed to be powerful sources of r-process matter and this has been proved thanks to the observation of the kilonova AT2017gfo, following the gravitational wave event GW170817 (Abbott et al., 2017; Watson et al., 2019). However, although both the r-process yields and the estimated rate of this phenomena seem to point towards MNS as the main r-process astronomical source, galactic chemical evolution models have problems to reproduce the r-process abundance pattern in the Galaxy if MNS are considered the only producers (Matteucci et al., 2014; Simonetti et al., 2019; Côté et al., 2019; Molero et al., 2021a). With the goal of better understanding both the r- and s- process production sites at low metallicity, we study the chemical evolution of Eu,

taken as a typical r-process element, and Ba abundances in 6 dSphs and 2 UFDs for which homogeneous abundances have been published by Reichert et al. (2020).

2. Model and nucleosynthesis prescriptions

We use a one-zone chemical evolution model with instantaneous and complete mixing of gas, able to follow the evolution of 31 elements, from H to Eu. Galaxies form by infall of primordial gas in a pre-existing and diffuse dark matter (DM) halo. Stellar lifetimes are taken into account, relaxing the instantaneous recycling approximation (IRA). The main sets of equations which describe the evolution with time of the gas mass in the form of the element i are:

$$\begin{aligned} \dot{M}_{\text{gas},i}(t) = & -\psi(t)X_i(t) + (\dot{M}_{\text{gas},i})_{\text{inf}} - \\ & + (\dot{M}_{\text{gas},i})_{\text{out}} + \dot{R}_i(t), \end{aligned} \quad (1)$$

The first term on the right-hand side of the equation is the rate at which chemical elements are subtracted by the ISM to be included in stars. The star formation rate (SFR) adopted is the Schmidt-Kennicutt law with $k = 1$ (Schmidt 1963; Kennicutt 1998). The second term is the rate at which chemical elements are accreted through infall of gas while the third term is the rate at which chemical elements are lost through galactic winds. Galactic winds develop when the thermal energy of the gas, heated by SN explosions and stellar winds, exceeds its binding energy (for details see Matteucci 1994; Bradamante et al. 1998; Vincenzo et al. 2014; Molero et al. 2022). The last term of the equation represents the fraction of matter that is returned by stars into the ISM in the form of the element i .

For all stars sufficiently massive to die in a Hubble time we adopted yields from Karakas (2010, for low and intermediate mass stars, LIMS), Kobayashi et al. (2006, for massive stars) and Iwamoto et al. (1999, for Type Ia SNe). A complete and detailed description of those yields can be found in Romano et al. (2010, see also Palla 2021).

For what it concerns heavy elements, s-process material is produced by LIMS during the AGB phase with yields from Busso et al. (2001), while r-process material is produced by both MNS and MRD-SNe. In our model NS binary systems consists of two $1.4M_{\odot}$ NS with progenitors in the $9 - 50M_{\odot}$ mass range. NS can merge with a delay time τ which can be either short (1 Myr) and constant (see Argast et al. 2004; Matteucci et al. 2014) or given by a delay time distribution (see Simonetti et al. 2019; Greggio et al. 2021). The yields of heavy elements (in this work Eu and Ba) from MNS have been obtained by assuming that there is a scaling relation between them and those of Sr (measured by Watson et al. 2019 in the reanalysis of the spectra of the kilonova AT2017gfo). On the other hand, in our model MRD-SNe are a subset of CC-SNe. In particular, we are assuming that 1 – 2% of all stars with mass in the $10 - 80 M_{\odot}$ are exploding as MRD-SNe and are producing heavy elements with yields from Nishimura et al. (2017, their model L0.75). Furthermore, it has been suggested that these events occur more frequently at low metallicities, because of the lower opacity that result in higher rotation rates and, as a consequence, stronger magnetic fields (see e.g., Brott et al., 2011, Thielemann et al., 2017). Therefore, we also test models in which the production of r-process elements from MRD-SNe is active only at metallicity $Z \leq 10^{-3}$, as suggested also in Winteler et al. (2012) and Cescutti et al. (2015).

3. Results

In this work we are focusing on the results obtained for Sagittarius dSph galaxy, for details on the other dSphs and UFDs we will refer to the main paper Molero et al. (2021b).

For Sagittarius dSph galaxy, we adopted the prescriptions of Mucciarelli et al. (2017) and of Vincenzo et al. (2015, who followed results of Lanfranchi et al., 2006). Moreover, we assumed a dark matter halo of mass $M_{DM} = 1.2 \times 10^8 M_{\odot}$ and an effective radius of the luminous component of the galaxy of $R_L = 1550 pc$ (Walker et al., 2009).

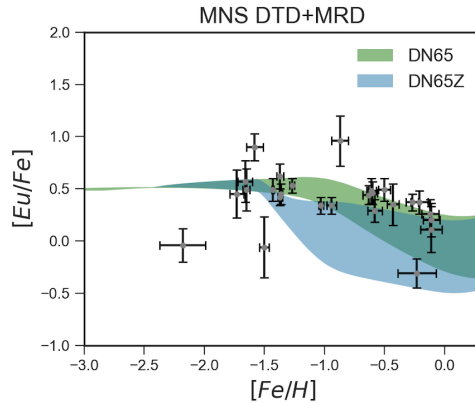


Fig. 1: Results for the [Eu/Fe] vs [Fe/H] pattern for Sagittarius dSph of models in which Eu is produced by both MNS with a DTD and MRD-SNe acting either at low Z (model DN65Z) or for all the range of metallicities (DN65Z).

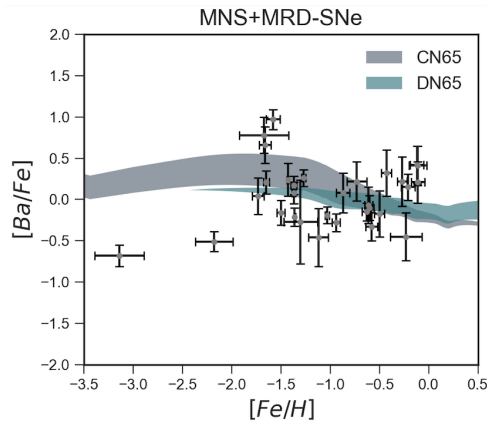


Fig. 2: Results for the [Ba/Fe] vs [Fe/H] pattern for Sagittarius dSph of models in which the r-process component of Ba is produced by MRD-SNe and MNS with either a DTD (model DN65) or with a constant delay time for merging (model CN65). The s-process Ba production comes from LIMS.

The SF history of Sagittarius is poorly constrained. By taking into account the work of de Boer et al. (2015), we assumed that stars formed efficiently ($\nu \sim 1 Gyr^{-1}$) during two different episodes of SF: the first occurring between 0 and 4 Gyr and the second occurring

between 4.5 and 7.5 Gyr. The SF is assumed to be null outside those time intervals.

In Figure 1, we report the observed [Eu/Fe] vs [Fe/H] pattern together with predictions of our models for Sagittarius dSph. Observationally, the evolution of [Eu/Fe] vs [Fe/H] shows a trend similar of that observed in the Galaxy. We can distinguish the plateau at low to intermediate metallicities and the decrease at higher [Fe/H]. In the Figure, we show results of models DN65 and DN65Z in which both MNS with a DTD and MRD-SNe can produce Eu. For both models the yield of Eu from MNS is in the $(3.0 \times 10^{-6} - 1.5 \times 10^{-5})M_{\odot}$ range, while that of MRD-SN is equal the one of Nishimura et al. (2017). The two models differ only for the range of metallicities in which MRD-SNe are active: in model DN65 they act for the whole range, while in model DN65Z they act only at low metallicities. Both models seem to be able to reproduce the main trend. If MNS were the only r-process elements producers, the model would have failed in reproducing data at low-metallicities (≤ -1.3 dex), due to the longer delay times for merging when a DTD is adopted. If also MRD-SNe are active, the lack of Eu at low metallicities is compensated. In the same way, when in model DN65Z MRD-SNe stop to produce Eu for metallicities higher than 10^{-3} , MNS can compensate. Both models are able to fit data, predicting a plateau at intermediate metallicities followed by a slight decrease at higher ones for Eu.

In Figure 2 we show results of models CN65 and DN65 in which heavy elements are produced by both MNS and MRD-SNe. In model CN65 we assume a short (1 Myr) and constant delay time for MNS, while in model DN65 a DTD is adopted. Both models are not able to reproduce the low data of [Ba/Fe] at low metallicities. In both cases, in fact, the production of r-process Ba sets in too early and a too high trend is produced at low [Fe/H].

4. Conclusions

In Molero et al. (2021b), we modelled the chemical evolution of seven dSph and two UFD galaxies in order to study the evolution of their Eu and Ba abundances. Here, we focused

on the results obtained for Sagittarius dSph and can be mainly summarized as follows: the most probable scenario for the production of Eu is that in which two sources are responsible for the production of r-process material. One source can be represented by MNS which merge with a DTD and a second source can be represented by MRD-SNe (which can be active either only at low or at all metallicities, without making any significant difference). The amount of Eu produced by each MNS event is in the $(3.0 \times 10^{-6} - 1.5 \times 10^{-5})M_{\odot}$ range, while that produced by MRD-SNe is in the range of the theoretical calculations of Nishimura et al. (2017) and equal to $4.69 \times 10^{-7}M_{\odot}$. However, this same scenario does not produce an agreement with the observed [Ba/Fe] vs [Fe/H] pattern, in particular at low metallicities where the production from MRD-SNe appears to be too enriched in Ba with respect to the observed abundances. Actually, the only way to reproduce those data at low metallicities would be if MNS with a DTD were the only producers of the r-process fraction of Ba, if also MRD-SNe participate to this process, the agreement with the data is lost.

Acknowledgements. M.M. thanks Deutsche Forschungsgemeinschaft through SFB 1245, which partially supported this work.

References

- Abbott B. P., et al., 2017, ApJ, 850, L40
- Argast D., Samland M., Thielemann F. K., Qian Y. Z., 2004, A&A, 416, 997
- Bradamante F., Matteucci F., D’Ercole A., 1998, A&A, 337, 338
- Brott I., et al., 2011, A&A, 530, A115
- Busso M., Gallino R., Wasserburg G. J., 1999, ARA&A, 37, 239
- Busso M., Gallino R., Lambert D. L., Travaglio C., Smith V. V., 2001, ApJ, 557, 802
- Cescutti G., Romano D., Matteucci F., Chiappini C., Hirschi R., 2015, A&A, 577, A139
- Côté B., et al., 2019, ApJ, 875, 106
- Cowan J. J., Sneden C., Lawler J. E., Aprahamian A., Wiescher M., Langanke K., Martínez-Pinedo G., Thielemann F.-K., 2019, arXiv e-prints, p. arXiv:1901.01410

- Frebel A., Beers T. C., 2018, *Physics Today*, 71, 30
- Greggio L., Simonetti P., Matteucci F., 2021, *MNRAS*, 500, 1755
- Halevi G., Mösta P., 2018, *MNRAS*, 477, 2366
- Iwamoto K., Brachwitz F., Nomoto K., Kishimoto N., Umeda H., Hix W. R., Thielemann F.-K., 1999, *ApJS*, 125, 439
- Karakas A. I., 2010, *MNRAS*, 403, 1413
- Kennicutt Robert C. J., 1998, *ApJ*, 498, 541
- Kobayashi C., Umeda H., Nomoto K., Tominaga N., Ohkubo T., 2006, *ApJ*, 653, 1145
- Lanfranchi G. A., Matteucci F., Cescutti G., 2006, *A&A*, 453, 67
- Matteucci F., 1994, *A&A*, 288, 57
- Matteucci F., Romano D., Arcones A., Korobkin O., Rosswog S., 2014, *MNRAS*, 438, 2177
- Molero M., Simonetti P., Matteucci F., della Valle M., 2021a, *MNRAS*, 500, 1071
- Molero M., et al., 2021b, *MNRAS*, 505, 2913
- Molero M., Matteucci F., Ciotti L., 2022, *arXiv e-prints*, p. arXiv:2210.11851
- Mösta P., Roberts L. F., Halevi G., Ott C. D., Lippuner J., Haas R., Schnetter E., 2018, *ApJ*, 864, 171
- Mucciarelli A., Bellazzini M., Ibata R., Romano D., Chapman S. C., Monaco L., 2017, *A&A*, 605, A46
- Nishimura N., Takiwaki T., Thielemann F.-K., 2015, *ApJ*, 810, 109
- Nishimura N., Sawai H., Takiwaki T., Yamada S., Thielemann F. K., 2017, *ApJ*, 836, L21
- Palla M., 2021, *MNRAS*, 503, 3216
- Reichert M., Hansen C. J., Hanke M., Skúladóttir Á., Arcones A., Grebel E. K., 2020, *A&A*, 641, A127
- Reichert M., Obergaulinger M., Eichler M., Aloy M. Á., Arcones A., 2021, *MNRAS*, 501, 5733
- Romano D., Karakas A. I., Tosi M., Matteucci F., 2010, *A&A*, 522, A32
- Schmidt M., 1963, *ApJ*, 137, 758
- Simonetti P., Matteucci F., Greggio L., Cescutti G., 2019, *MNRAS*, 486, 2896
- Thielemann F. K., et al., 2011, *Progress in Particle and Nuclear Physics*, 66, 346
- Thielemann F.-K., Eichler M., Panov I., Pignatari M., Wehmeyer B., 2017, *Making the Heaviest Elements in a Rare Class of Supernovae*. p. 1843, doi:10.1007/978-3-319-21846-5_81
- Vincenzo F., Matteucci F., Vattakunnel S., Lanfranchi G. A., 2014, *MNRAS*, 441, 2815
- Vincenzo F., Matteucci F., Recchi S., Calura F., McWilliam A., Lanfranchi G. A., 2015, *MNRAS*, 449, 1327
- Walker M. G., Mateo M., Olszewski E. W., Peñarrubia J., Evans N. W., Gilmore G., 2009, *ApJ*, 704, 1274
- Watson D., et al., 2019, *Nature*, 574, 497
- Winteler C., Käppeli R., Perego A., Arcones A., Vasset N., Nishimura N., Liebendörfer M., Thielemann F. K., 2012, *ApJ*, 750, L22
- Wosley S. E., Heger A., 2006, *ApJ*, 637, 914
- de Boer T. J. L., Belokurov V., Koposov S., 2015, *MNRAS*, 451, 3489